Article

TRANSACTIONS OF THE INSTITUTE OF MEASUREMENT & CONTROL

Transactions of the Institute of Measurement and Control
35(8) 1085–1093

DOI: 10.1177/0142331213481841
tim.sagepub.com
SAGE

Control of a pneumatic drive using electronic pressure valves

Željko Šitum

Abstract

The primary task of the electronic pressure (E/P) valves is to control the pressure continuously in different industrial automation processes. Their use in pneumatic drives allows regulating pressures in both cylinder chambers and so it is possible to achieve a direct force controlled actuator. Additionally to the force control, position control of the pneumatic actuator using E/P valves has been presented. A dynamic model for control purposes of the process has been derived, followed by the PID controller tuned according to damping optimum criteria. The control algorithms have been experimentally verified on an industrial cylindrical rod-less actuator controlled by two E/P valves. The control performances are comparable with the set-up with proportional directional control valves (servo-valves). Based on the experimental results, it can be concluded that these valves have potential for successful implementation in industry for position and force control applications.

Keywords

Design, digital control, dynamic modelling, electronic pressure valves, experiments, PID, pneumatics

Introduction

Pneumatic driving systems are usually used in manufacturing processes where it is necessary to achieve a device that is inexpensive, clean, reliable and simple for realization. They have found widespread application in the field of industrial automation for 'pick-and-place' positioning problems. However, for free positioning tasks, pneumatic drives are quite difficult to control. This complexity arises primarily from the phenomena associated with the use of compressible fluid and friction effects, which deteriorate the time response and positional accuracy of the pneumatic servo-actuation system. Over the years, some other motion technologies have been commonly used for flexible positioning operations, mainly based on costly electromechanical systems for lighter loads and hydraulic drives for heavy loads. However, the development of proportional directional control (PDC) valves created a pneumatic servo-technology. Despite the problems in control of pneumatically powered drives, engineering practice has shown that they offer in many cases competitive cost/performance characteristics. Using the proportional valves, a continuous feedback control can be obtained. Thus it is possible to perform flexible, fast and precise positioning tasks of pneumatic actuators. As a result, much research has been carried out, dealing with the development of various control concepts for pneumatic drives for motion or force control (Liu and Bobrow, 1988; Richer and Hurmuzlu 2000a, 2000b, and bibliographies therein; Smaoui et al., 2006; Surgenor and Vaughan, 1997; Xiang and Wikander, 2004). In many studies, relatively expensive proportional servo-valves have been used, which, however, give the best results, especially in applications where precise positioning and smooth motion are required. Some adequate control algorithms such as pulse-width modulation (PWM) techniques enable low-cost on/off solenoid valves to be used as an admissible substitute for costly proportional valves in pneumatic servo applications (e.g. Ahn and Yokota, 2005; Messina et al., 2005; Shih and Ma, 1998; Varseveld and Bone, 1997).

In this work, the actuator is controlled by two E/P valves. They consist of a combination of electro-pneumatic pilot valves, pressure regulators and piezo-resistive pressure sensors for achieving internal pressure feedback. The main difference between these valves related to the manually controlled pressure regulator is the replacement of the control spring by a proportional solenoid that generates a force proportional to the electric command signal. They are used in those applications where electrical control is required to act directly on a change of pressure or force. These valves have standard three-way configuration with supply, outlet and vent ports. An amplifier is built into the valve and enables an easy electrical connection with a control device. They have a multi-step or linear pressure outputs depending on the electrical command signal from the control device. These valves are usually used in different automation processes requiring continuous pressure control, for example tank pressure control, control of

Automatic Control and Robotics, Faculty of Mechanical Engineering and Naval Architecture, University of Zagreb, Zagreb, Croatia

Corresponding author:
Željko Šitum, Automatic Control and Robotics, Faculty of Mechanical Engineering and Naval Architecture, University of Zagreb, I. Lučića 5, 10000 Zagreb, Croatia.
Email: zeljko.situm@fsb.hr

cylinder force, tension control, counterbalancing control, nozzle flow control, etc. (Wang et al., 2007). However, controlling the pressure in the cylinder chambers and achieving an external position feedback, these valves can also be used in realization of an electro-pneumatic servo-drive for positioning tasks (Hashimoto and Ishida, 2000; Sorli et al., 2004). With such characteristics, E/P valves have a potential for force as well as for position control applications.

In this paper, a control-oriented mathematical model of pneumatic actuator controlled by E/P valves is derived, followed by a design of the PID controller tuned according to damping optimum criteria. Then, a short description of the experimental system is given. Finally, the experimental results of cylinder pressure (or force) control, as well as position control of pneumatic servo-drive using E/P valves, are presented.

Process modelling

In this section, a dynamic model for control purposes of the cylindrical actuator system controlled by two E/P valves is derived. To obtain a transfer function that provides a relation between the position of the piston x and the command signal u on the valve, first the relation between the piston position and the cylinder relative pressure will be derived, and then the relation between the cylinder relative pressure and the control signal. It is well known that conventional PID controllers may have difficulties in controlling non-linear systems with hysteresis and significant friction effects such as controlled pneumatic drives. To reduce the impact of these non-linear effects, an offset signal to the PID output will be added so that the controller can react to the error more effectively in order to bring the system to the desired set-point value. The offset signal will have a value to overcome the static friction force, and in case of the cylinder in motion, the friction will be presented with a simplified model of viscous friction.

Relation between piston position and cylinder pressure

The motion equation of piston due to applied pressure difference p_{L} may be given in the following form:

$$\ddot{x} = \frac{1}{m}(A\,p_{\mathrm{L}} - F_{\mathrm{f}}) \tag{1}$$

where the load pressure $p_{\mathrm{L}} = p_{\mathrm{A}} - p_{\mathrm{B}}$ is the pressure differential across the piston, m is the load and piston mass ($m = m_{\mathrm{p}} + m_{\mathrm{L}}$), A is the annulus area of the piston, F_{f} is the friction force of the cylinder and x is the position of the actuator.

The friction force in the above equation can be described by a well-known Stribeck static characteristic:

$$F_{\mathrm{f}}(\dot{x}) = \left[F_{\mathrm{c}} + (F_{\mathrm{s}} - F_{\mathrm{c}})\,e^{-|\dot{x}/\dot{x}_{\mathrm{s}}|^{\delta_{\mathrm{s}}}} + k_{\mathrm{f}}\,\dot{x}\right] \cdot \mathrm{sgn}(\dot{x}) \tag{2}$$

where F_{c} and F_{s} are Coulomb friction force and breakaway force respectively, $\dot{x}_{\mathrm{s}}$ is the so-called Stribeck speed, δ_{s} is the Stribeck exponent and k_{f} is the viscous friction coefficient.

Assuming that the piston is in motion (i.e. friction is mainly described by viscous friction only), the transfer function as the ratio of the piston position and the pressure difference in the cylinder chambers, which from Equation (1) can be expressed as follows:

$$\frac{x(s)}{p_{\mathrm{L}}(s)} = \frac{A}{s\,(m\,s + k_{\mathrm{f}})} \tag{3}$$

Relation between cylinder pressure and control signal

The cylinder air pressure dynamics (assuming isothermal process within the cylinder) might be described by the following expression (Beater, 2007):

$$\dot{p}_{\mathrm{L}} = -\frac{p_s A}{V/2}\,\dot{x} + \frac{p_s}{V/2}\frac{p_0}{\rho_0}\,K_v\,u \tag{4}$$

where p_{s} is the supply pressure, p_0 and ρ_0 are the ambient pressure and air density respectively, A is the piston cross-section, V is the total air volume, $\dot{x}$ is the piston speed, K_v is the valve coefficient and u is the valve command voltage. The first term on the right-hand side of Equation (4) describes the effect of the volume change and the second part the effect of the valve flow on the pressure change, which means that the mass flow rate depends linearly from the valve command signal ($\dot{m} = p_s\,K_v\,u$).

The pressure difference p_{L} is directly proportional to the cylinder applied force F (i.e. $F = A \cdot p_L$). By rewriting the transfer function given in Equation (3) in terms of piston speed $\dot{x}(s)$ and substituting it into Equation (4), the following expression for the pressure build-up in the cylinder is obtained:

$$\dot{p}_{\mathrm{L}} = -\frac{2\,p_s A}{V}\,\frac{p_L A}{m\,s + k_{\mathrm{f}}} + \frac{2\,p_s}{V}\frac{p_0}{\rho_0}\,K_v\,u \tag{5}$$

or written in polynomial form as:

$$m\,s^2 p_L + k_{\mathrm{f}}\,s\,p_L + \frac{2\,p_s A^2}{V}p_L = \frac{2\,p_s}{V}\frac{p_0}{\rho_0}\,K_v\,(m\,s + k_{\mathrm{f}})\,u \tag{6}$$

The continuous-time transfer function from above equation is given as follows:

$$\frac{p_L(s)}{u(s)} = \frac{K_v \frac{p_0}{\rho_0 A^2}(m\,s + k_{\mathrm{f}})}{\frac{m\,V}{2p_s A^2}\,s^2 + \frac{k_{\mathrm{f}}\,V}{2p_s A^2}\,s + 1} = \frac{C_0\,(T_D\,s + 1)}{\frac{1}{\omega_0^2}\,s^2 + \frac{2\zeta}{\omega_0}\,s + 1} \tag{7}$$

where: $\omega_0 = \sqrt{\frac{2p_s A^2}{m\,V}}$ is the natural frequency, $\zeta = \frac{k_{\mathrm{f}}}{2}\sqrt{\frac{V}{2p_s A^2 m}}$ is the damping ratio, $C_0 = K_v \frac{p_0}{\rho_0 A^2}$ is the model gain and $T_D = \frac{m}{k_{\mathrm{f}}}$ is the 'lead' time constant.

Pole-zero analysis of the transfer function (7) shows the closeness of the zero and one pole, especially in the case of drive without load, indicating the possibility of reducing the order of the system. The transfer function as the ratio of the

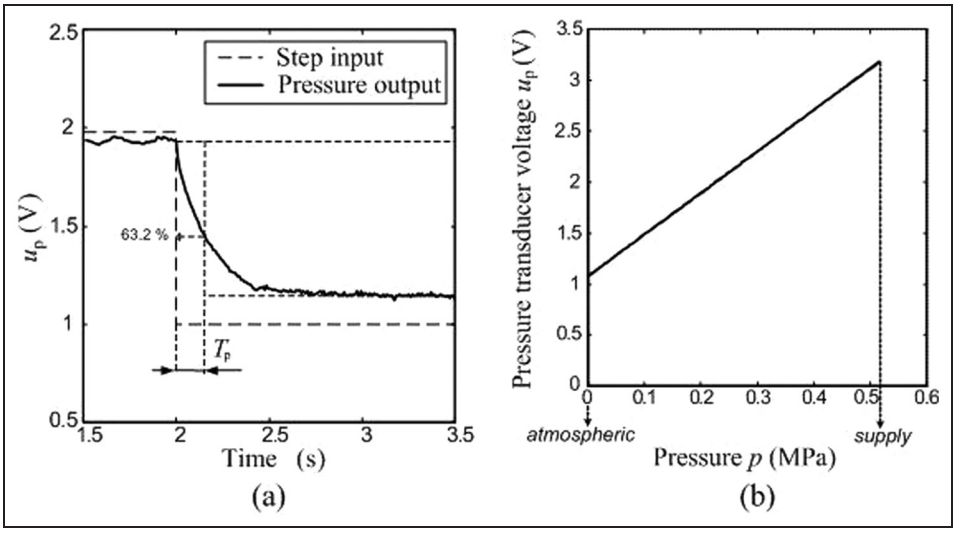

Figure 1. (a) Pressure transient response; (b) characteristic of the pressure transducer.

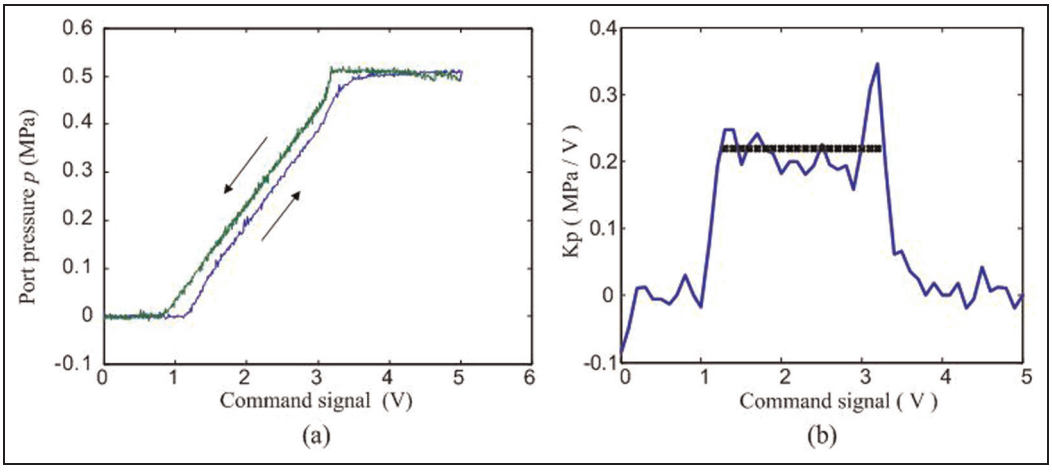

Figure 2. Calibration of the pressure transducer: (a) static characteristic; (b) slope of the calibration curve.

relative pressure in the cylinder chambers and the control signal on the valve is also obtained from the experimentally measured pressure response on a step command input (Figure 1a). The measured output u_p is the voltage obtained on the pressure transducer. The pressure transient response has an aperiodic form, and can be approximated by a first-order lag term as follows:

$$\frac{p_L(s)}{u(s)} = \frac{K_p}{T_p s + 1} \tag{8}$$

where K_p is the transfer gain and T_p is the time constant. From the reference step change illustrated in Figure 1(a), the time constant of the process can be approximated with a numerical value $T_p \approx 0.1\,5$ s. According to the pressure transducer characteristic shown in Figure 1(b), the relative pressure p in the cylinder chamber can be expressed by the following relation:

$$p\ [\text{MPa}] = 0.248\ u_p\ [\text{V}] - 0.273 \tag{9}$$

where u_p is the measured output voltage of the pressure transducer.

The forward gain K_p will be estimated from experimentally obtained calibration curve of the valve, shown in Figure 2(a), which presents the relative pressure outlet versus the input voltage signal. The forward gain K_p is valid for the linear part of the calibration curve shown in Figure 2(a). The calibration curve was obtained by measuring voltage on the pressure transducer for varying command signal (from 0 to 5 V and vice versa with an increment of 0.01 V) and with the conversion from the voltage signal to the relative pressure using Equation (9). The experiment was conducted for the cylinder in mid-stroke because the lowest stability margin tends to occur just around the mid-stroke position (Pu et al., 1992).

By using the relation from Equation (9), the measured voltage signal was converted into cylinder relative pressure.

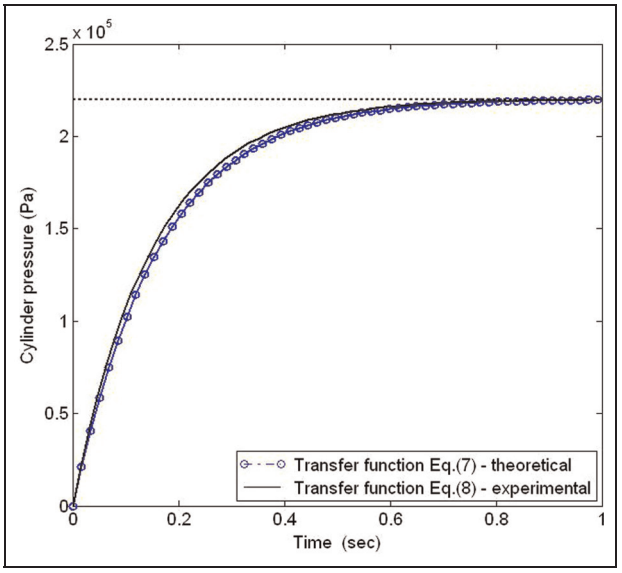

Figure 3. Pressure build-up in the cylinder.

The curve has a hysteretic shape, and it includes saturation non-linearity. This non-linearity will have a greater impact in control of force than in the task of position control. Namely, due to the feedback signal from the position transducer, the controller will form a control signal and thus the pressure in the cylinder chambers to achieve the least error positioning. For control voltage signal, higher then approximately 3.2 V, the static curve enters into saturation caused by limited supply pressure ($p_s \approx 0.52$ MPa). Thus, the usable voltage signal u during the system control will be in the range 1.1–3.2 V (linear part of the static characteristic). The forward gain K_p is defined as the ratio between the cylinder load pressure p_L and the control voltage u for the steady-state conditions. On the linear part of the static curve, it can be approximated numerically by the value $K_p \approx 0.22$ MPa/V (Figure 2b).

A comparison of simulation responses of the cylinder air pressure dynamics model obtained in Equation (7) and the experimentally identified model for the case of system without load given with Equation (8) showed very similar behaviour of pressure response on the step command input (Figure 3). Therefore, further in this paper, the pressure dynamics model given in Equation (8) will be used, the parameters of which were experimentally identified in this section. The model parameters used for simulation were taken from Table 1.

Plant transfer function

Considering the piston position x as an output and the command voltage signal from the control device u as an input, the process transfer function is obtained by multiplying the relations given in Equations (3) and (8) as follows:

$$G_p(s) = \frac{x(s)}{u(s)} = \frac{A K_p}{s(m s + k_f)(T_p s + 1)} \tag{10}$$

Table 1.

System parameters	Symbol	Nominal value
Cross-sectional area	A	$1.767 \cdot 10^{-4}$ m^2
Volume of the cylinder	V	$8.835 \cdot 10^{-5}$ m^3
Supply pressure	p_S	$5.2 \cdot 10^5$ pa
Ambient pressure	p_0	1.10^5 pa
Initial mass of piston	m_P	0.91 Kg
Load mass	m_L	3.98 kg
Viscous friction coeff.	K_f	65 Ns/m
D/A converter gain	K_{DA}	$2.44 \cdot 10^{-3}$ V
A/D converter gain	K_{AD}	204.8 V^{-1}
Measuring system gain	K_m	20 V/m
Valve coefficient	K_v	$0.825 \cdot 10^{-7}$ kg/sPaV
Sampling time	T	0.01 s

The nominal system parameters required for modelling and controller design are summarized in Table 1. These parameters were obtained on the basis of manufacturer's component specification, via experiment and through numerical calculation (Šitum et al., 2004).

Controller design

The controller parameters are optimized according to the damping optimum analytical design method (Zäh and Brandenburg, 1987). Calculating the closed-loop system characteristic polynomial, and equating it with the forth-order damping optimum characteristic polynomial yields the equations for the controller parameters.

The continuous-time transfer function of the process given in Equation (10) can be rearranged in the following form:

$$G_p(s) = \frac{b_0}{s(1 + a_1 s + a_2 s^2)} \tag{11}$$

where $b_0 = A K_p / k_f$, $a_1 = m/k_f + T_p$ and $a_2 = m T_p / k_f$. Using a modified I-PD (set-point-on-I-only) structure of PID controller (Åström and Wittenmark, 1984), given in Figure 4, the transfer function of the closed-loop system is found to be:

$$G_{cl}(s) = \frac{K_R b_0}{K_R K_m b_0 (1 + T_I s + T_I T_D s^2) + T_I s^2 (1 + a_1 s + a_2 s^2)} \tag{12}$$

Placement of the classical PID controller in the control error path may cause an extensive control effort and output response overshoot. This is due to the introduction of controller zeros in the transfer function of the closed-loop control system. On the other hand, in the modified I-PD controller form, controller zeros do not exist in the closed-loop transfer function. This controller structure can be viewed as the conventional PID controller structure with the prefilter $G_f(s) = 1/(1 + T_I s + T_I T_D s)$ placed in the set-point path (Šitum et al., 2004).

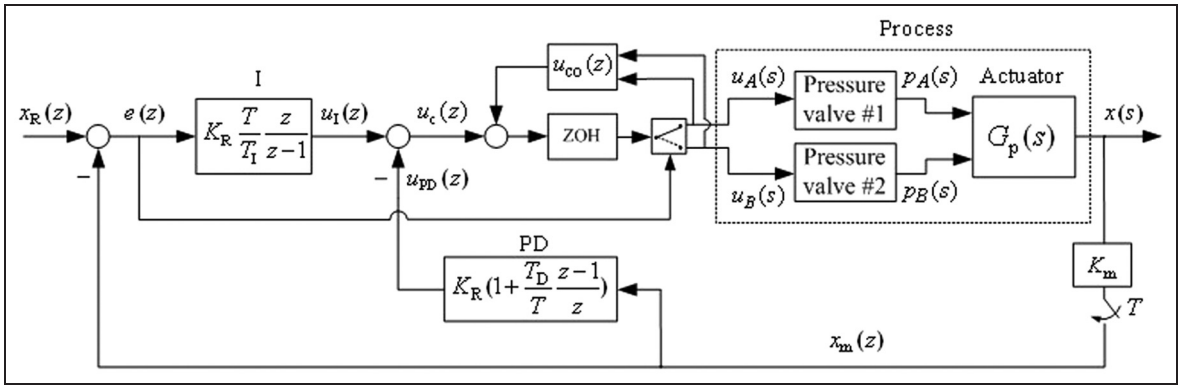

Figure 4. Block diagram for position control.

For the sake of controller design simplification, the delay time from the D/A converter is not included here because of relatively large time constant of the process.

The characteristic polynomial for the fourth-order system written in terms of the damping optimum criteria has the form as follows:

$$A(s) = 1 + T_e s + D_2 T_e^2 s^2 + D_2^2 D_3 T_e^3 s^3 + D_2^3 D_3^2 D_4 T_e^4 s^4 \quad (13)$$

where T_e is the equivalent time constant of the closed-loop system and D_2, D_3 and D_4 are the characteristic ratios. If all of the characteristic ratios D_i are set to the optimal value 0.5, the application of the damping optimum results in the so-called quasi-aperiodic step response, with a small overshot and rise time ($\sigma_m = 6\ \%$, $t_{100\,\%} = 1.8\,T_e$) (Naslin, 1968).

From the transfer function given in Equation (12), the characteristic polynomial of the closed-loop system can be expressed as:

$$A(s) = 1 + T_I s + \frac{T_I(1 + K_R K_m b_0 T_D)}{K_R K_m b_0} s^2 + \frac{T_I a_1}{K_R K_m b_0} s^3 + \frac{T_I a_2}{K_R K_m b_0} s^4 \quad (14)$$

By equating the coefficients of the damping optimum of the characteristic polynomial in Equation (13) to the corresponding coefficients of the characteristic polynomial of the closed-loop system in Equation (14), the PID controller parameters are found to be:

$$K_R = \frac{a_1}{K_m b_0 T_e^2 D_2^2 D_3};\ T_I = \frac{a_2}{a_1}\frac{1}{D_2 D_3 D_4};\ T_D = D_2 T_e\left(1 - \frac{D_2 D_3 T_e}{a_1}\right) \quad (15)$$

It is obvious that the equivalent time constant T_e is equal to the integral time constant T_I. The system response is dominantly determined by the lower characteristic ratios D_2 and D_3. Non-dominant characteristic ratio D_4 can be calculated by equating the coefficient a_4 from Equation (14) to the corresponding coefficient of the characteristic fourth-order polynomial of the damping optimum in Equation (13) and has the following values:

$$D_4 = \frac{a_2}{K_R K_m b_0 D_2^3 D_3^2 T_e^3} \quad (16)$$

In order to obtain an aperiodic response, the most dominant characteristic ratio D_2 should be set to the value $D_2 = 0.37$, while keeping the less dominant characteristic ratios to the value 0.5 (Naslin, 1968). By using parameters of the process given in Table 1, the numerical values of the modified PID controller are obtained as follows: $K_R = 10.45$, $T_I = 0.138$s, $T_D = 0.043$s for the unloaded drive and $K_R = 0.98$, $T_I = 0.525$s, $T_D = 0.109$s for the loaded drive. In both cases, the non-dominant characteristic ratio D_4 has a value of around 0.5.

A block diagram of the position control system with modified PID controller structure is shown in Figure 4. When the relative velocity is approximately zero, the friction is largely responsible for a steady-state error. The system is in the so-called 'stick' regime. By using E/P valves, a relatively precise value of pressure in cylinder chamber for a commanded signal can be set. This possibility can be used for detection of the breakaway friction force, i.e. for the start of the drive motion. The experimental tests for detecting the value of the static friction force were conducted under both unloaded and loaded conditions (the load was $m_L = 3.8$ kg deadweight) and the results are illustrated in Figure 5. At the moment when velocity of the drives is greater than zero (or the moment of drives' breakaway) the applied force can be supposed as the static friction force. The command signals u_{co}, which are necessary for starting of the drive motion, are added to the control algorithm by means of an offset value regarding the control error and drive motion direction. This contribution will support the reduction of negative effects of non-linear phenomena in pneumatic systems, and the use of I-PD form of the regulator ensures a fairly good positioning accuracy. According to Figure 5, it can be estimated that the static friction force in the case of the unloading drive is $F_s = 35$ N (and the corresponding offset voltage signal $u_{co} = 1.85$ V) and in the case of the loading cylinder is $F_s = 44$ N (and the corresponding offset voltage signal $u_{co} = 2.25$ V). The control signal from the controller u_c, which also included an offset signal u_{co}, is sent to the proportional valves. Which valve is activated depends on the sign of the control error.

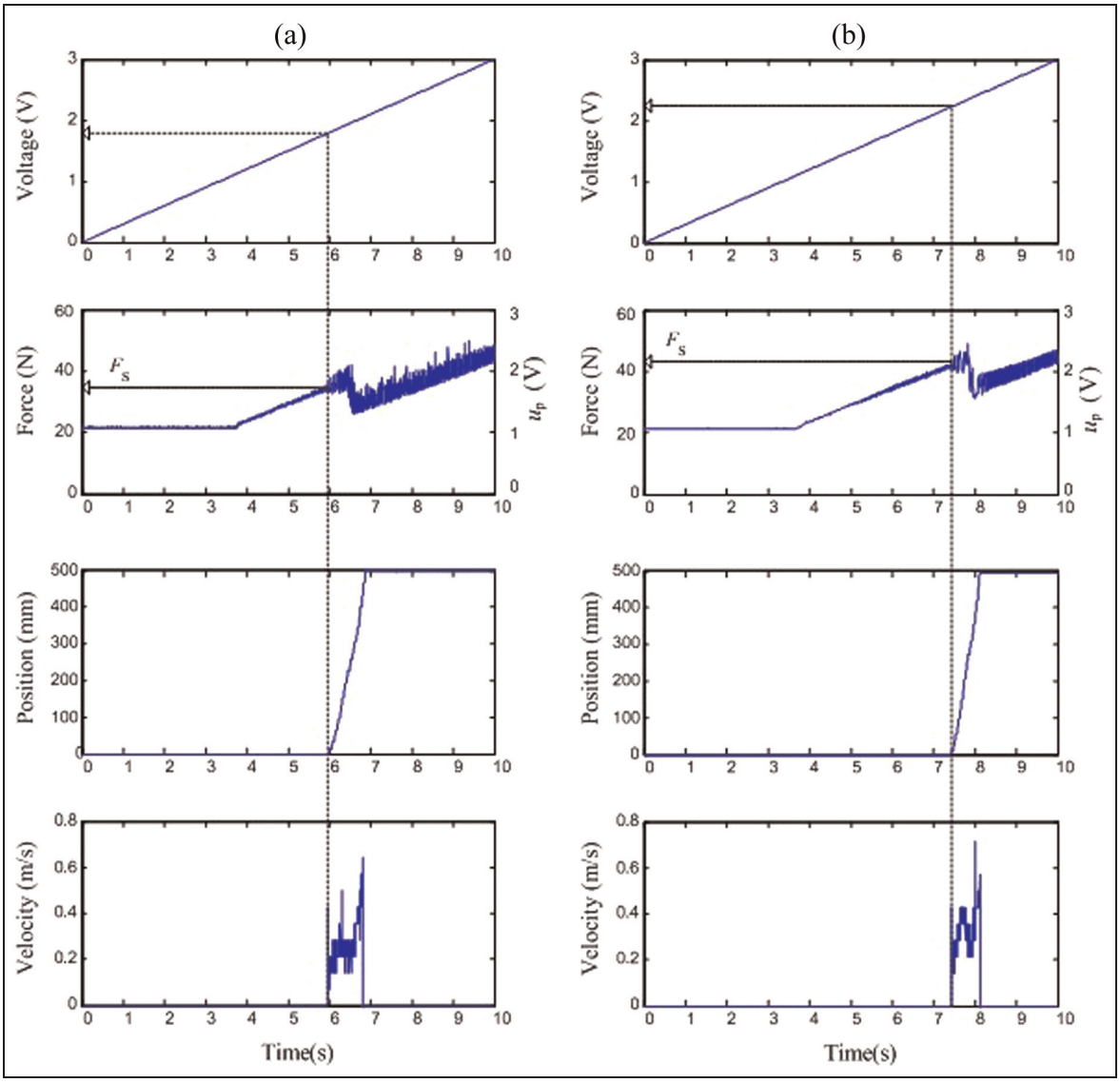

Figure 5. Detection of the static friction force: (a) without load; (b) with load m_L=3.8 kg.

Description of pneumatic servo-system

Experiments were performed on the test apparatus, a schematic description of which is illustrated in Figure 6(*a*), while a photo of the laboratory equipment is shown in Figure 6(*b*). The actuator used in the experiment is a rodless double-acting cylinder with a stroke length of 500 mm and inner diameter of 15 mm. A mass load of $m_L = 3.8$ kg (a cast iron block) can be placed on the cylinder slider. A linear potentiometer, with a specified repeatability of ± 0.25 mm and a linearity of 0.05% of full scale, attached to the cylinder slider is used to measure piston position. Two E/P valves are attached to the cylinder chambers. They are controlled by means of a voltage signal in the range 0–5 V from the control computer, which allows the realization of pressure difference in the cylinder chambers. Three pressure transducers are available to measure the pressure evolution in each cylinder chamber and also the pressure of the air supply. The control software is coded in C language and the feedback control algorithms are performed on a PC via a data-acquisition card. The experimental equipment also includes a PDC valve (Festo MPYE-5 1/8 HF-010B) and two on/off solenoid valves (SMC EVT307-5D0-01F), which are not used in this work. The test system was built in-house for educational laboratory use.

Experimental results

As mentioned before, the E/P valves are usually used for cylinder pressure (or force) control, where they convert an input electric signal into outlet pressure. One such example of pressure control in the cylinder chamber when the input voltage is changed in a stepwise manner is illustrated in Figure 7. Pressure response was measured using the pressure transducer

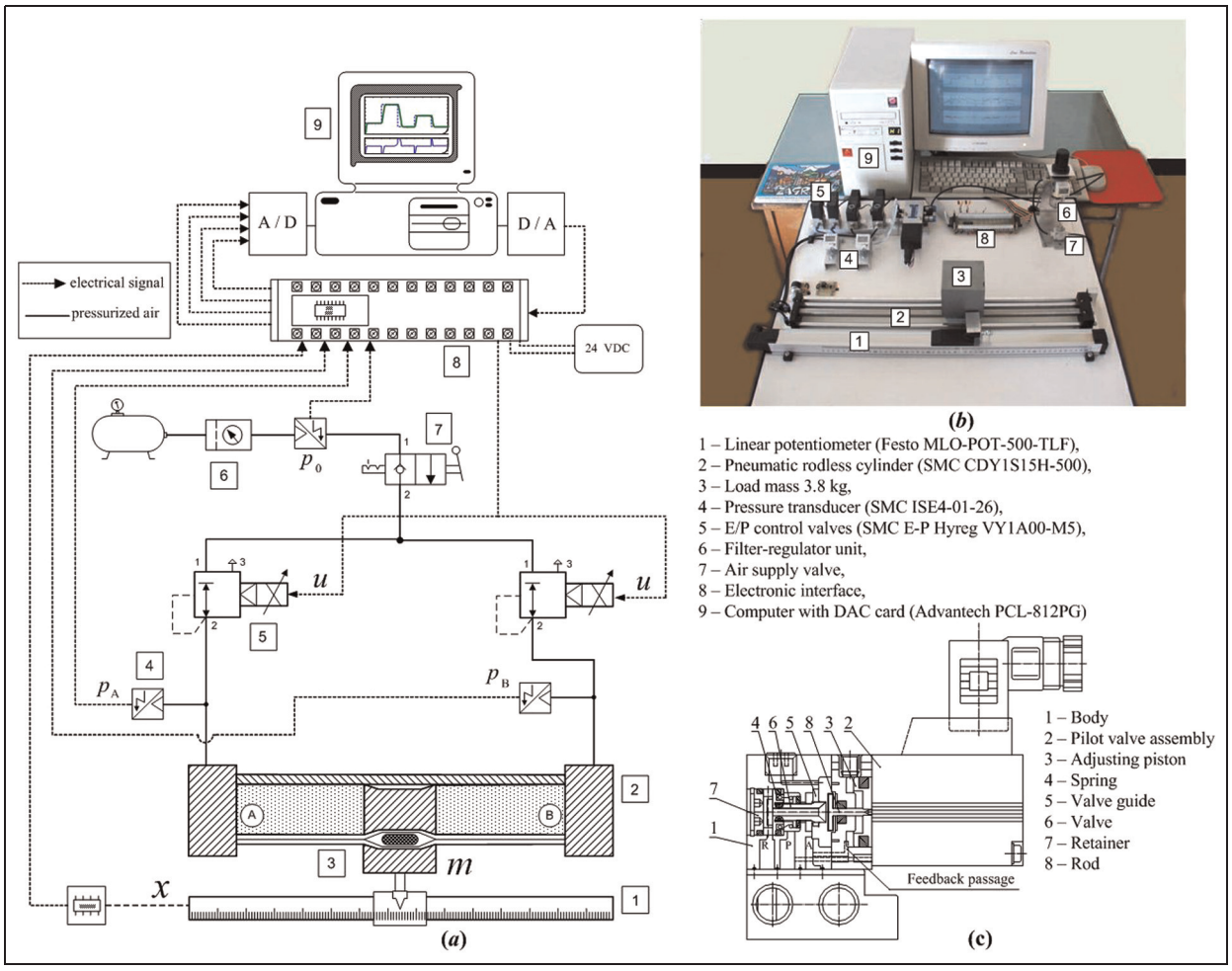

Figure 6. Experimental set-up: (a) Schematic drawing of the control system; (b) photo; (c) E/P valve.

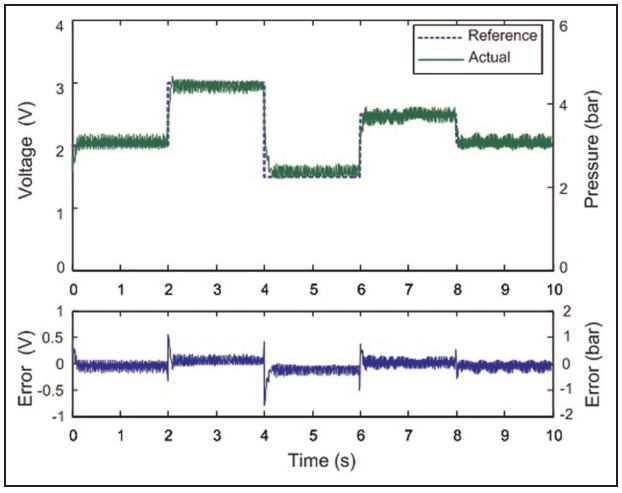

Figure 7. Pressure control of pneumatic drive in an open loop.

and is presented as an output voltage u_p. Applying the expression for the conversion of cylinder pressure from the measured sensor voltage, which is given in Equation (9), the corresponding pressure in the cylinder chamber is also shown in Figure 7 on the right side of the y-axis. The application of these valves in industrial environments may be accompanied by certain specific problems associated with significant noise in the measured pressure signal due to the way the E/P valves operate. Namely, when a command signal is given, the valve output pressure gives feedback to the internal control circuit by an internal pressure transducer and, depending on the control error, the outlet port connects to the supply or the vent port. Permanent moving of the pressure control piston inside the valve causes the high-frequency oscillations of the outlet pressure, which is manifested as a noise inherent in the data measured by the external pressure sensor.

The experiments for the actuator position control were also conducted to confirm the effectiveness of the proposed controller described earlier. Experimental tests were performed in case of the unloaded and loaded drives. The obtained experimental results for the pneumatic servo-drive position control to a square-wave reference signal are shown in Figure 8. The PID controller tuned according to damping optimum criteria was used in the control algorithm. The experiments demonstrate a relatively fast response with no overshoot, both for unloaded and loaded control systems. On

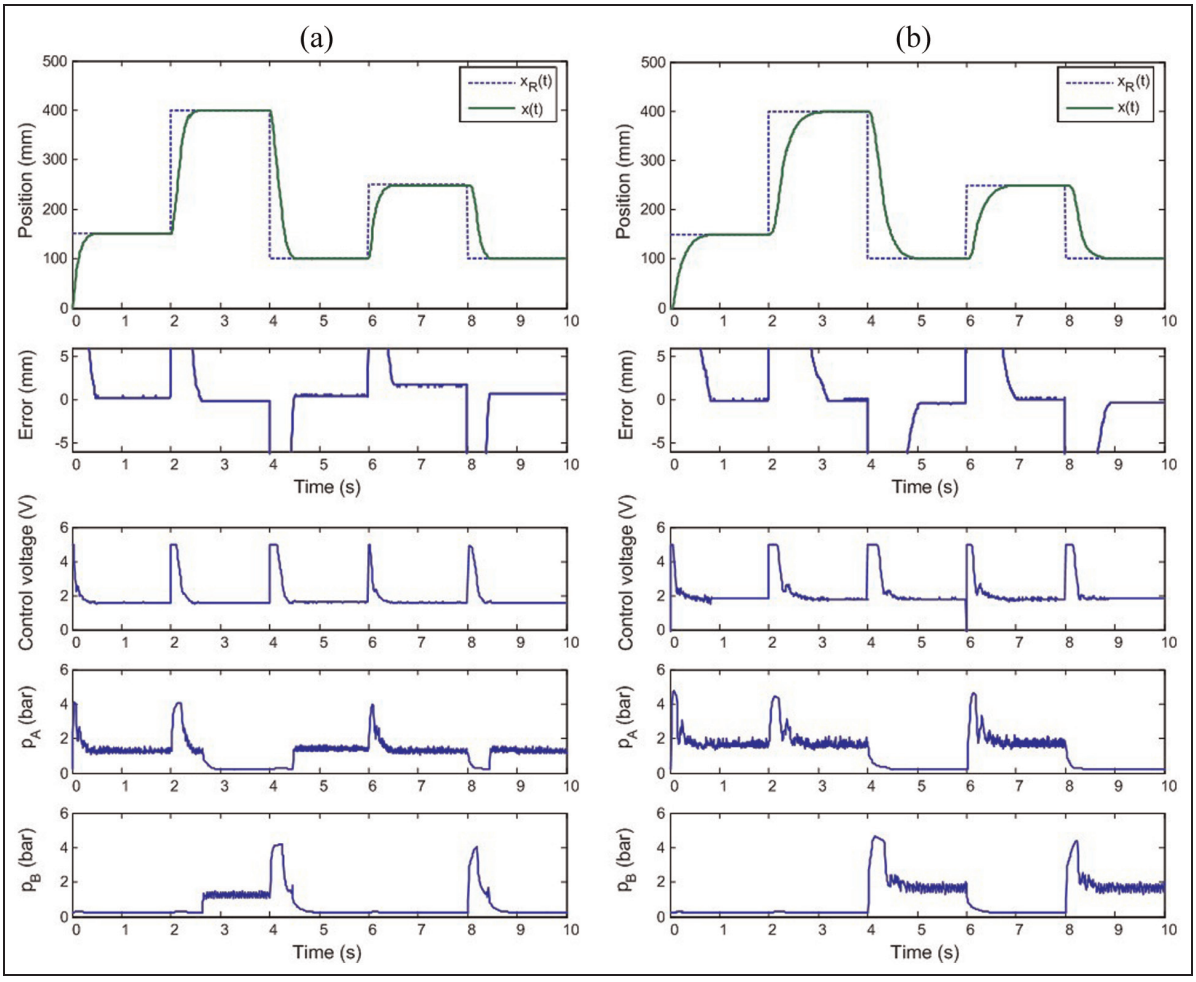

Figure 8. Position control of pneumatic drive: (a) without load; b) with load m_L=3.8 kg.

average, this control strategy enables the steady-state error of within ±1 mm, which compares well with previous results for a PDC valve (Šitum and Petrić, 2001). For the case of the loaded drive, the responses of the system were found to be slower due to the longer period of the control signal saturation.

Conclusion

A simplified control oriented dynamic model of a pneumatic cylinder controlled by two E/P valves has been derived. The process parameters are analysed and experimentally identified. Based on the model of the process, the PID controller has been optimized according to the damping optimum criteria. The proposed control method has been applied for a pneumatic position control system. The experimental results indicate that the proposed analytical controller design method can also be effectively used for position control of the pneumatic servo-system for less demanding industrial applications. Simplicity of the control algorithms allows them to be implemented on the standard micro-controller systems.

This raises the question of whether E/P valves have some advantages over the PDC valves that are usually used for this purpose. Looking at the economic aspect, two E/P valves are roughly the same cost as one PDC valve, so the use of pressure valves can hardly have an economic advantage. The settling time of the system with these two types of valves is approximately equal, but using PDC valves in servo applications can achieve slightly better positioning accuracy when it is necessary to ensure accurate positioning in a wider range of possible values. Standard E/P valves are mainly used in industry where electrical control is required to act directly on a change of pressure or force. However, the E/P valves have the potential for hybrid force/position control applications, giving designers new possibilities in system regulation.

References

Ahn K and Yokota S (2005) Intelligent switching control of pneumatic actuator using on/off solenoid valves. *Mechatronics* 15: 683–702.

Åström KJ and Wittenmark B (1984) *Computer Controlled Systems*. Englewood Cliffs, NJ: Prentice-Hall International.

Beater P (2007) Pneumatic Drives: System Design, Modelling and Control. Berlin: Springer-Verlag.

Hashimoto T and Ishida Y (2000) An adaptive I-PD controller based on frequency domain system identification. *ISA Transactions* 39: 71–78.

Liu S and Bobrow JE (1988) An analysis of a pneumatic servo system and its application to a computer controlled robot. *ASME Journal of Dynamic Systems, Measurement, and Control* 110: 228–235.

Messina A, Giannoccaro N and Gentile A (2005) Experimenting and modelling the dynamics of pneumatic actuators controlled by the pulse width modulation (PWM) technique. *Mechatronics* 15: 859–881.

Naslin P (1968) *Essentials of Optimal Control*. London: Iliffe Books Ltd.

Pu J, Weston RH and Moore PR (1992) Digital motion control and profile planning for pneumatic servos. *ASME Journal of Dynamic Systems, Measurement, and Control* 114: 634–640.

Richer E and Hurmuzlu Y (2000a) A high performance pneumatic force actuator system: Part I – Nonlinear mathematical model. *ASME Journal of Dynamic Systems, Measurement, and Control* 122: 416–425.

Richer E and Hurmuzlu Y (2000b) A high performance pneumatic force actuator system: Part II – Nonlinear controller design. *ASME Journal of Dynamic Systems, Measurement, and Control* 122: 426–434.

Shih MC and Ma MA (1998) Position control of a pneumatic cylinder using fuzzy PWM control method. *Mechatronics* 8: 241–253.

Šitum Ž and Petrić J (2001) Modeling and control of servopneumatic drive. *Strojarstvo* 43(1–3): 29–39.

Šitum Ž, Pavković D and Novaković B (2004) Servo pneumatic position control using fuzzy PID gain scheduling. *ASME Journal of Dynamic Systems, Measurement, and Control* 126: 376-387.

Smaoui M, Brun X and Thomasset D (2006) A study on tracking position control of an electropneumatic system using backstepping design. *Control Engineering Practice* 14(8): 923–933.

Sorli M, Figliolini G and Pastrorelli S (2004) Dynamic model and experimental investigation of a pneumatic proportional pressure valve. *IEEE/ASME Transactions on Mechatronics* 9: 78–86.

Surgenor BW and Vaughan ND (1997) Continuous sliding mode control of a pneumatic actuator. *ASME Journal of Dynamic Systems, Measurement, and Control* 119: 578–581.

Varseveld RB and Bone GM (1997) Accurate position control of a pneumatic actuator using on/off solenoid valves. *IEEE/ASME Transactions on Mechatronics* 2: 195–204.

Wang XS, Cheng YH and Peng GZ (2007) Modeling and self-tuning pressure regulator design for pneumatic-pressure-load systems. *Control Engineering Practice* 15: 1161–1168.

Xiang F and Wikander J (2004) Block-oriented approximate feedback linearization for control of pneumatic actuator system. *Control Engineering Practice* 12(4): 387–399.

Zäh M and Brandenburg G (1987) The extended damping optimum – an analytical optimization method for control systems with numerical polynomial (in German). *at-Automatisierungstechnik* 35: 275–283.